Unclassified
SECURITY CLASSIFICATION OF THIS PAGE

DTIC FILE COPY

2

REPORT DOCUMENTATION PAGE

1a. REPORT SECURITY CLASSIFICATION Unclassified	1b RESTRICTIVE MARKINGS None
2a. SECURITY CLASSIFICATION AUTHORITY AD-A217 631	3. DISTRIBUTION/AVAILABILITY OF REPORT Approved for public release and sale. Distribution unlimited.
4. PERFORMING ORGANIZATION REPORT NUMBER(S) ONR Technical Report No. 17	5. MONITORING ORGANIZATION REPORT NUMBER(S)
6a. NAME OF PERFORMING ORGANIZATION University of Utah 6b. OFFICE SYMBOL (If applicable)	7a. NAME OF MONITORING ORGANIZATION
6c. ADDRESS (City, State, and ZIP Code) Department of Chemistry Henry Eyring Building Salt Lake City, UT 84112	7b. ADDRESS (City, State, and ZIP Code)
8a. NAME OF FUNDING/SPONSORING ORGANIZATION Office of Naval Research 8b. OFFICE SYMBOL (If applicable)	9. PROCUREMENT INSTRUMENT IDENTIFICATION NUMBER N00014-89-J-1412
8c. ADDRESS (City, State, and ZIP Code) Chemistry Program, Code 1113 800 N. Quincy Street Arlington, VA 22217	10. SOURCE OF FUNDING NUMBERS PROGRAM ELEMENT NO. / PROJECT NO. / TASK NO. / WORK UNIT ACCESSION NO

11. TITLE (Include Security Classification)
Raman Spectroscopy of the Liquid-Solid Interface: Monolayer and Bilayer Adsorption of Pyridine on Silica

12. PERSONAL AUTHOR(S)
S. F. Simpson and J. M. Harris

13a. TYPE OF REPORT	13b. TIME COVERED	14. DATE OF REPORT (Year, Month, Day)	15. PAGE COUNT
Technical	FROM 7/89 TO 7/90	January 30, 1990	30

16. SUPPLEMENTARY NOTATION

17. COSATI CODES			18. SUBJECT TERMS (Continue on reverse if necessary and identify by block number)
FIELD	GROUP	SUB-GROUP	Surface energetics; adsorption at liquid/solid interface

19. ABSTRACT (Continue on reverse if necessary and identify by block number)

Attached.

20. DISTRIBUTION/AVAILABILITY OF ABSTRACT ☒ UNCLASSIFIED/UNLIMITED ☐ SAME AS RPT ☐ DTIC USERS	21. ABSTRACT SECURITY CLASSIFICATION Unclassified
22a NAME OF RESPONSIBLE INDIVIDUAL Dr. Robert J. Nowak	22b TELEPHONE (Include Area Code) (202) 696-4410 22c OFFICE SYMBOL

DD FORM 1473, 84 MAR

83 APR edition may be used until exhausted.
All other editions are obsolete.

SECURITY CLASSIFICATION OF THIS PAGE
Unclassified

OFFICE OF NAVAL RESEARCH

Grant No: N00014-89-J-1412

R&T Code 413a005---03

Technical Report No. 17

Raman Spectroscopy of the Liquid-Solid Interface: Monolayer and Bilayer Adsorption of Pyridine on Silica

Prepared for publication in Journal of Physical Chemistry

by

S. F. Simpson and J. M. Harris

Departments of Chemistry
University of Utah
Salt Lake City, UT 84112

January 30, 1990

RAMAN SPECTROSCOPY OF THE LIQUID-SOLID INTERFACE: MONOLAYER AND BILAYER ADSORPTION OF PYRIDINE ON SILICA

S. F. Simpson and J. M. Harris*
Department of Chemistry
University of Utah
Salt Lake City, UT 84112

ABSTRACT

Raman spectra of pyridine adsorbed at a silica-solution interface are reported. A flow-through sample cell is employed to control the illuminated surface area of the particulate sample and to minimize background from solution phase species. The technique is applied to study the adsorption of pyridine onto silica gel from carbon tetrachloride solution. Spectroscopic adsorption isotherms are acquired with sufficient precision to allow monolayer and bilayer forms of adsorbed pyridine to be distinguished and quantified. The monolayer form adsorbs with proton transfer from the silica surface, where the degree of proton transfer decreases uniformly with increasing surface coverage. A Frumkin model fits the monolayer isotherm data and provides an estimate of the decrease in free energy of adsorption with increasing surface coverage. The bilayer isotherm exhibits a concentration threshold which could only be fit by assuming that its energy of adsorption depends strongly on monolayer coverage. The accumulation of this pyridine bilayer appears to play a role in stabilizing the charge density of ion pairs in the monolayer.

INTRODUCTION

In order to better understand the molecular interactions responsible for adsorption and chromatographic retention of molecules from liquids onto silica and chemically-modified silica surfaces, a number of studies have recently appeared in which fluorescent spectroscopic probes are used to provide information about the structure of the liquid-solid interface [1-5]. These investigations have provided information about the polarity and heterogeneity of the interfacial environment and the organization and distribution of surface-bound ligands. To better determine the molecular basis of the surface interactions which are responsible for these phenomena, acquisition of vibrational spectra of molecules at the silica-solution interface is a particularly desirable experimental goal, the achievement of which poses several difficulties. With infrared spectroscopy, the intense absorption of the silica network and surface silanols precludes routine acquisition of spectra below 1200 cm^{-1}. In addition, these amorphous materials typically exhibit high fluorescence and Rayleigh scattering backgrounds which hinder the detection of Raman scattering. Clearly, the development of experimental methods to measure vibrational spectra of surface-adsorbed or surface-bound probe molecules at the silica-solution interface is important to investigate interactions which are responsible for adsorption or binding to the surface.

Recent advances in multichannel detectors coupled with higher power lasers have increased the viability of Raman spectroscopy as a structural probe in surface chemistry [6-9]. In this work, we exploit these advances to acquire vibrational spectra of molecules at the silica-solution interface. As an initial study, we have investigated the adsorption of pyridine at the carbon tetrachloride-porous silica interface. The frequencies of the two symmetric

ring stretching modes of pyridine shift characteristically to higher frequency when the molecule is adsorbed to the silica surface. The intensity of these bands can be plotted as a function of pyridine concentration in the mobile phase to generate spectroscopic isotherms of both the adsorbate monolayer and bilayer. Previous Raman spectroscopic investigations of pyridine adsorption to silica provide background for the present experiment [10,11]. Witke [10] followed pyridine adsorption to silica by adding known quantities of Aerosil (pyrogenic silica) to a stirred solution of pyridine in carbon tetrachloride. Raman spectra were collected from a volume of solution which was considerably larger than the volume of the dispersed particles. As a result, the spectra contain significant interference from solution phase species; the data were fit to a Langmuir isotherm which was found to be an adequate model within the error in the measurement. Sayed and Cooney [11] also carried out a Raman investigation of the adsorption of pyridine on Cabosil, also a pyrogenic silica, where spectra were acquired from hand-pressed pellets of silica that were immersed in solvent. A small amount of pyridine was introduced onto the surface of the solvent and allowed to diffuse through bulk solution and interact with the silica surface. The pyridine, initially adsorbed to the silica surface, was found to occupy Bronsted sites on the silica, and evidence of a slow, laser-assisted desorption of pyridine was also presented.

In contrast to these previous experiments, the present work examines samples of porous silica which are contained in a flow cell through which solutions are pumped to equilibrate with the silica surface. Raman spectra are collected by illuminating the sample cell with red laser excitation to avoid fluorescence background from the silica; Raman scatter in the near-infrared is detected using a charge-coupled-device detector. The benefit of this approach

over previous methods is that the number of surface sites which are examined is controlled by the constant packing density of silica in the flow cell, while the surface concentration of the adsorbate is governed by the adsorption equilibrium and the bulk concentration of adsorbate in the solution reservoir. The resulting control over adsorbate signal is sufficient to readily identify small deviations from linear isotherm behavior, to detect the accumulation of a physisorbed bilayer, and to quantify the density of adsorbed molecules on the surface.

EXPERIMENTAL SECTION

Chemicals. The adsorption studies were performed on Partisil 10, a porous xerogel from Whatman, having an average particle diameter of 10 μm, a surface area of 323 m^2g^{-1}, and a mean pore diameter of 96 Å. The silica was dried for 12 hours at 110 ^oC under 1 millitorr vacuum prior to use. Carbon tetrachloride (EM Science, Omnisolv) was used without further purification, and pyridine (Fisher Scientific) was stored over molecular sieves. Solutions of varying pyridine concentration between 0.96 mM and 1.91 M in carbon tetrachloride were prepared using standard volumetric techniques.

Raman Spectrometry. Laser excitation was provided by a krypton ion laser (Coherent, Innova 90K, Palo Alto, CA) operating at 676.4 nm. Red excitation was used in order to minimize the fluorescence background from the silica. Interfering plasma lines from the excitation beam were removed with a filter consisting of two Pellin Brocca prisms in combination with a variable aperture. The power of the laser beam at the sample was 30 mW.

A standard, two lens arrangement consisting of an F/1.4 aspherical lens and an F/6 plano-convex lens was used to collect and focus the scattered

radiation onto the slits of a triple monochromator (Model 1877, Spex Industries, Edison, New Jersey). The spectrometer was calibrated using the Raman spectra of liquid pyridine and indene [12]. Raman scatter was detected using a charge-coupled-device (CCD) (Thomson, Model CSF THF7882CDA) contained in a cryogenic dewar (Model CH210, Photometrics, Ltd., Tucson, AZ) and cooled to -115 ^{o}C. The two-dimensional (384 channel x 576 channel) CCD was positioned such that the spectrum was dispersed along the horizontal (576 channel) axis to maximize spectral resolution. The CCD was operated so that photoelectrons were binned (summed) along the vertical axis of the chip to minimize readout noise. A spectral region of 350 cm^{-1} was covered with a resolution of 0.6 cm^{-1}/channel by the detection system in this configuration. Data acquisition and readout electronics (Model CE200 and Model CC200, Photometrics, Ltd.) were slaved to a microcomputer (Model D, Leading Edge, Canton, MA) via standard IEEE-488 communications for data storage and subsequent spectral analysis and plotting.

Procedure. In these experiments, it was desired to collect Raman spectra under conditions where the surface area under examination would be constant and the exposure to adsorbate from solution could be controlled. The silica gel sample was, therefore, contained in an optically accessible flow-through sample cell. The sample cell consisted of a 1.5 mm i.d. precision bore quartz tube supported in a (1 cm x 1 cm) brass cuvette as previously described [10,13]. Two holes on adjacent sides of the cuvette permitted the use of standard 90^{o} Raman excitation-collection geometry. The exit end of the quartz tube was fitted with a frit which contained the silica gel while pyridine-carbon tetrachloride solutions were flowed through the silica using a high pressure pump (Model 110A, Beckman, Fullerton, CA). The flow cell assembly was mounted

on a 3-d translation stage which facilitated alignment in the laser beam.

After the quartz tube was packed with silica, the cell was assembled and carbon tetrachloride was pumped for 15 minutes at a flow rate of 0.3 mL/min to pack the gel and to displace air from the porous solid. Both the collection optics and the sample cell were adjusted during this time by monitoring the 459 cm^{-1} band of carbon tetrachloride to obtain maximum Raman signal output. Once the Raman signal had been optimized, the monochromator sine bar was positioned to observe the ring stretching vibration region of pyridine. No further adjustments were made to the apparatus during the experiment.

Solutions were equilibrated with the silica surface, beginning with the most dilute pyridine concentration and continuing in order of increasing concentration. Each new test mixture was pumped through the silica for a minimum of 10 minutes prior to data collection to ensure that equilibrium between the solid surface and solution had been reached. Spectra were collected for each solution using two minute integration times (total excitation energy of 3.6 J). Raman spectra were also obtained for the pyridine-carbon tetrachloride solutions without the presence of the gel to determine the relative intensities of the two pyridine bands in solution and to test for shifts in the solution phase Raman band frequencies as a function of concentration.

Data Analysis. In order to construct the spectroscopic adsorption isotherms, peaks in the Raman spectra were modelled using a Gaussian bandshape to obtain peak area and position parameters. The best fit was determined by minimizing the chi-squared statistic [14]; due to significant background scatter from the silica, the relative intensity differences across the spectrum were small so that the weighting factors for shot-noise were set equal to a

constant. Fits of the experimental adsorption isotherms from peak area data to various isotherm models were conducted using nonlinear least squares, in which the chi-squared statistic was again used to evaluate the goodness of fit.

Generation of adsorption isotherms. Adsorption isotherms for both the monolayer and bilayer were prepared by plotting relative surface coverage of the appropriate species as a function of pyridine concentration in solution. Previous gas-solid adsorption studies of pyridine on silica have demonstrated the intensity of the band appearing at ca. 1010 cm^{-1} (ν_1) to be proportional to the amount of pyridine adsorbed in the first monolayer [15]. Therefore, the relative coverage for the monolayer was calculated from the area of the peak at ν_1. Since the spectrum of physisorbed pyridine in an adsorbed bilayer appears to be identical to that of neat pyridine liquid [15] (which is the same as pyridine in carbon tetrachloride solution), the total signal intensity at 992 cm^{-1} is due to Raman scattering of molecules in the bulk solution plus the scattering from the physisorbed bilayer. At high pyridine concentrations, the total signal is dominated by Raman scattering from molecules in bulk solution. Therefore, the Raman signal attributable to the surface physisorbed species was obtained by extrapolation of the linear region of the 992 cm^{-1} band intensity versus concentration to obtain the solution-phase pyridine signal in absence of adsorbed pyridine; this solution-phase signal was then subtracted point-by-point from total 992 cm^{-1} signal at each pyridine concentration to obtain an estimate of the physisorbed or bilayer pyridine contribution. This procedure was checked by measuring the 992 cm^{-1} scattering intensity versus pyridine concentration for solutions of pyridine in carbon tetrachloride over the same concentration range; this plot resulted in a linear calibration curve passing through the origin.

RESULTS AND DISCUSSION

Raman spectra of pyridine at the silica-CCl_4 interface. Studies of pyridine adsorbed to metal oxide surfaces indicates that the interaction with the surface generally occurs through the lone pair electrons on the nitrogen heteroatom in the ring [16-18]. The strength of this interaction varies with the surface and results in either: hydrogen bonding between pyridine and hydroxyl groups on the metal oxide surface, Bronsted interactions in which a proton is transferred from an acidic surface hydroxyl group to the heterocycle to form pyridinium ion, or Lewis interactions in which the pyridine binds to a Lewis acid site at the oxide surface. Indicative of the specific type of interaction is a characteristic shift in the vibrational frequency of both the totally symmetric ring breathing mode and the trigonal symmetry ring stretching mode of the molecule [19]. The totally symmetric ring mode undergoes the largest shift in frequency and is therefore the most diagnostic with regard to the chemical environment experienced by the molecule at the oxide surface. The ratio of the scattering intensities of these modes is also characteristic of the type of interaction.

To assess the interactions of pyridine with silica in contact with carbon tetrachloride, Raman spectra taken of a packed bed of silica gel at equilibrium with pyridine solution concentrations ranging from 1.9 mM to 1.9 M are presented in Figure 1. For the lowest concentrations of pyridine, the band center of the totally symmetric ring breathing mode appears at a frequency, $\nu_1 = 1012\ cm^{-1}$, while the frequency of the trigonal symmetry ring mode initially appears at $\nu_{12} = 1034\ cm^{-1}$. The ratio of the scattering intensity of the trigonal mode to that of the totally symmetric mode is initially 0.25. The frequency, ν_1, of the initially adsorbed pyridine, together with the

observed intensity ratio of 0.25, is strongly characteristic of pyridinium ion [11,19]. The assignment of the initial adsorbate interactions with the surface as Bronsted is consistent with previous findings for low concentrations of pyridine at a silica-carbon tetrachloride interface [11].

As the pyridine concentration is increased, surface coverage becomes more complete, as shown by the concomitant growth in intensity of the ν_1 mode. A limiting intensity is reached at approximately 100 mM pyridine, which signals the formation of a monolayer. At solution concentrations exceeding this value, additional Raman bands from pyridine begin to appear at frequencies ν_1 = 992 cm^{-1} and ν_{12} = 1030 cm^{-1} which are indistinguishable from pyridine in free solution. Since these bands overlap with those of the initial adsorbate, determining the intensities and center frequencies of the four bands was carried out by fitting the spectra to Gaussian band shapes. The fit of the spectra was constrained by determining several peak parameters in advance. Raman spectra of pyridine in carbon tetrachloride solution were acquired to determine the intensity ratio of the trigonal ring mode (ν_{12}) to the totally symmetric ring breathing mode (ν_1) to be 0.91 $\pm$ 0.03; this value was used to constrain the relative intensity of these two bands for the "solution-like" species. The mean frequencies and band widths of both ν_1 and ν_{12} for pyridine in solution were found to be invariant with concentration; these were used as additional constraints on the spectrum of the solution-like species. Finally, the band widths surface species were allowed to vary, but were found to be invariant with concentration. The number of variable parameters in the model was reduced, by these constraints, to only seven: two band center frequencies, widths, and intensities for the initial adsorbate, and one intensity parameter for the solution-like species. An example of the quality of fit is shown

Figure 2 for pyridine at a concentration of 96 mM.

From the fit of the overlapped spectra, the center frequency of the totally symmetric ring vibration of the initial adsorbate can be determined over the range of monolayer accumulation. As the solution concentration of pyridine and the surface coverage are increased, ν_1 of the adsorbate shifts to lower frequency. Figure 3 shows a plot of ν_1 versus the relative surface coverage, the latter being estimated from the relative intensity of the band. As seen in the figure, ν_1 shifts monotonically to lower frequency over the entire range of surface coverage to a final value of 1008 cm-1 which is reached upon completion of the monolayer. These data are consistent with an average reduction in the degree of proton transfer with increasing the surface coverage. This behavior could be due to a distribution of surface silanol acidities, which would lead to a distribution of band frequencies that would broaden as weaker sites are occupied at higher coverages. We observe no detectable change in the peak width of ν_1, however, with increasing surface coverage ruling out an energetic distribution of adsorption sites. The band shift together with uniformity in peak width suggests, rather, that the extent of charge transfer between pyridine and the silica surface decreases uniformly with pyridine surface coverage, most likely due to electrostatic interactions (charge repulsion) between adjacent surface dipoles. Further evidence for these kinds of interactions at the silica surface is apparent in the isotherm results.

Monolayer adsorption isotherm. In order to gain a better understanding of the energetics of pyridine adsorption to silica, the Raman intensity (peak area) of the totally symmetric mode for the initial adsorbate was plotted as a function of solution concentration of pyridine, as shown in Figure 4. The

results were compared to various models for surface adsorption. The data in Figure 4 (a) exhibit a rapid gain in adsorbate coverage at low concentrations, followed by a more gradual approach to monolayer completion. This shape corresponds qualitatively to the Type I Brunauer isotherm that is associated with the theory of Langmuir [20,21]; as a consequence, we attempted to fit the data initially to a simple Langmuir model, of the form:

$$\theta/(1 - \theta) = \beta C \qquad (1)$$

where θ is the fractional coverage, β is the adsorption equilibrium constant, and C is the molar concentration of the adsorbent approximating its activity in solution. Solving this equation for the fractional coverage versus solution concentration gives:

$$\theta = \beta C/(1 + \beta C) \qquad (2)$$

If the Raman scattering cross section of the adsorbate is unaffected by surface coverage, then θ can be estimated from the relative intensity of Raman scatter. This is a reasonable assumption since the peak width was found not to vary with coverage and the vibrational frequency changes by only 0.4%. The fit of the data to Equation 2 is shown in Figure 4, where a plot with a logarithmic concentration axis, Figure 4(b), is included to illustrate the full range of the fit. The best fit value of the equilibrium constant is $\beta = 2.2 \times 10^2$ $\underline{M}^{-1}$. The fit of the monolayer isotherm data to the Langmuir equation were met with limited success, particularly as seen in the Figure 4(b) showing the full range of solution concentrations used to optimize the parameters. A reciprocal plot, C/θ versus C, yielded a straight line expected for Langmuir adsorption [10]. Such a plot is, however, very insensitive to the quality of fit since the linearity of response is dominated by concentration in the numerator of the dependent variable. These results demonstrate that care must be taken when

interpreting data plotted in the reciprocal form of the Langmuir equation.

Strict adherence to a Langmuir adsorption model precludes the following three conditions: (1) adsorption of more than layer of molecules at the surface, (2) surface site heterogeneity, or (3) interactions between adsorbed molecules. Deviations from Langmuir adsorption behavior can be attributed to the presence of one or more of these conditions. The first condition can be ruled out by the unique frequency shift of the symmetric ring vibration of pyridine associated with proton transfer from silica to the adsorbate. Observing the intensity of this spectroscopic feature assures that one is following adsorbed pyridine which is intimately associated with the surface. At amorphous solid surfaces, the second condition would not generally hold and the simple Langmuir picture of adsorption becomes complicated due to a distribution of adsorption energies often modeled by the Fruendlich isotherm or other empirical equation [22]. The lack of detectable band broadening of the ν_1 vibrational mode of pyridine as a function of increasing surface coverage, despite the significant shift in vibrational frequency, infers that surface heterogeneity plays a lesser role in this system than do interactions between adsorbed molecules. As discussed above, the shifts in the adsorbate vibrational frequency with coverage together with the uniformity of Raman band widths appear to indicate a uniform decrease in the degree of proton transfer between adsorbate and the surface with increasing coverage.

To account for the corresponding effect of adsorbate interactions on the adsorption equilibrium, we have used a Frumkin isotherm model [23,24], where the equilibrium constant is modified from its value at low coverages, β_o, by an exponential factor which assumes a linear dependence of the standard free energy of adsorption with surface coverage:

$$\theta/(1 - \theta) = \beta_o C \exp(2g\theta) \quad (3)$$

The parameter g in the exponential argument is a proportional to the variation of the adsorption energy with coverage; using the sign convention of Frumkin [24], the parameter is less than zero when the adsorbate interactions are repulsive and greater than zero when they are attractive.

The experimental monolayer adsorption data for pyridine are replotted in Figure 5, along with a best fit to a Frumkin isotherm. The quality of fit, as estimated by the reduced chi-square statistic (corrected for the degrees of freedom in the fit [14]), is smaller by a factor 0.13 compared to the Langmuir model. The probability that the improvement in precision is an artifact of the particular data sampled is, according to an F-test, less than 3%. A duplicate measurement of the isotherm reproduced the relative intensities within 5% and showed equivalent improvement in fit by the Frumkin model. From these results, the value of the equilibrium constant in the limit of zero coverage (where the isotherm becomes Langmuir-like) is $\beta_o = 4.3\ (\pm 0.2) \times 10^2\ \underline{M}^{-1}$, and the dependence of the adsorption energy on coverage is given by a factor $g = -0.82\ (\pm 0.02)$. The sign of this factor indicates a reduction in the adsorption equilibrium constant with increasing coverage, characteristic of repulsive forces between the adsorbed molecules. This behavior is easily rationalized in view of the coverage-dependent lowering of the proton transfer between the silica and the adsorbate inferred from the symmetric ring mode vibrational frequencies. The nearly linear shift in the frequency with coverage could relate to the excellent fit to a Frumkin model, which assumes a linear change in the adsorption energy with coverage.

The magnitude of the change in the adsorption energy with coverage can also be estimated from these results. The free energy of adsorption is equal

to the difference in the chemical potential of the adsorbate in the adsorbed state versus that in free solution, $\Delta G_a = \mu_a - \mu_s$. Using the Langmuir definition for the standard state of the adsorbate [25], $\theta = 0.5$, the standard free energy of adsorption may be obtained from $\Delta G_a^o = -RT \ln [\theta/(x(1-\theta))]$, where x is the mole fraction of adsorbate in solution. Using this definition, the difference in the standard free energy of adsorption for the Frumkin isotherm compared to the Langmuir-like, limiting behavior at low surface coverages can be obtained from the value of the parameter g in Equation 3 [26], $\Delta(\Delta G_a^o) = -(g\ RT) = 0.48$ kcal/mole. This value of the adsorbate repulsive energy at half-coverage seems quite realistic in light of electrostatic forces between surface dipoles, created by proton transfer from the surface and the adsorbate, at intermolecular distances which are as small as 8 Å (see below).

Pyridine bilayer isotherm. Further evidence for the electrostatic interaction between adjacent surface dipoles in the adsorbate monolayer is apparent in the accumulation of a second layer of adsorbed pyridine at the liquid/solid interface. The build-up of this physisorbed layer is not as obvious as the pyridine monolayer described above, since the vibrational frequencies are not shifted compared with free solution. The concentration dependence of the intensity of the solution-like Raman scatter from the symmetric ring mode at 992 cm^{-1} reveals a non-linear region at low concentrations, corresponding to the accumulation of surface excess pyridine; see Figure 6. The lack of a shift in the vibrational frequency of this band compared to free solution indicates that neither proton transfer nor hydrogen bonding, between the surface and this adsorbed pyridine layer, is present.

The linear response at high concentrations in Figure 6 is indicative of Raman scatter from pyridine in the solution phase. The slope of the line

relating scattered light intensity and solution concentration was determined by a linear least squares fit to the highest three concentration points. A linear model for the solution phase behavior was generated using this slope and a zero intercept; this model was subtracted point-by-point from the total 992 cm^{-1} intensity to obtain an estimate of the signal from surface excess pyridine. A plot of these results is shown in Figure 7.

While the monolayer isotherm reaches half-coverage of the surface at a relatively low solution concentration of pyridine, 5.6 mM, the bilayer isotherm requires 30-fold greater pyridine concentration, 0.16 M, to reach the half-coverage level. The higher required solution concentration does not derive from a smaller equilibrium constant for adsorption since the rise in the bilayer coverage is very steep beyond a threshold solution concentration. A simple model which can account for this behavior is one where the energy of adsorption for the bilayer depends on the monolayer coverage. This model is proposed in light of (1) the double-layer charging by proton transfer to the pyridine monolayer and (2) the repulsive interactions between these molecules inferred from the vibrational frequency shifts and the fit to a Frumkin isotherm. The 5.5-fold larger dielectric constant [27] of pyridine, $\epsilon = 12.3$, compared to the carbon tetrachloride solvent, $\epsilon = 2.2$, could clearly account for a bilayer of pyridine being attracted to the interface, as the charged monolayer accumulates. The higher dielectric constant of the bilayer would stabilize the ionic species in the interface and reduce the repulsive interactions between the adsorbed ion pairs. A Frumkin-like expression where the energy of adsorption of the bilayer depends linearly on the monolayer coverage is given by:

$$\theta_b/(1 - \theta_b) = \beta_b C \exp(2g_b\theta) \qquad (4)$$

where θ_b and θ are fractional bilayer and monolayer coverages, respectively, β_b is the equilibrium constant for the bilayer adsorption in the limit of no monolayer coverage, and g_b is the variation of the bilayer adsorption energy with monolayer coverage. A best fit of the bilayer data to this equation is also shown in Figure 7, where $\beta_b = 1.8\ (\pm 0.1) \times 10^{-8}\ \underline{M}^{-1}$ and $g_b = 10.5\ (\pm 0.2)$, which corresponds to strong, attractive interactions between the bilayer and monolayer.

The bilayer data are quite consistent with the Frumkin-like isotherm of Equation 4. The model captures the adsorption behavior throughout the concentration range of the experiment, including the minimal accumulation of molecules in the bilayer at low solution concentrations followed by a fast rise in accumulation beyond a threshold concentration. Other isotherms were tested on this data, including Equation 3, with no success. None could reproduce the threshold behavior observed in the data. Examining the parameters which fit Equation 4 to the data, a minimal intrinsic attraction of molecules into the bilayer at small monolayer coverages is indicated by the very small value of β_b. This outcome seems reasonable since the bilayer experiences no direct interaction with the silica surface. The very large value of g_b, in contrast, shows the stabilizing influence of the bilayer on the ion pairs in the monolayer. The accumulation of monolayer adsorbate strongly controls the adsorption equilibrium for the bilayer. At half-coverage by the monolayer, $\theta = 0.5$, the bilayer adsorption free energy changes, from its low concentration limit, by $\Delta(\Delta G) = -(g_b\ RT) = -6.2\ (\pm 0.1)$ kcal/mole. Given the large solvation energies for transferring ions to media of higher dielectric constant [28], the magnitude of this result is not surprising. At the same half-coverage condition, recall that the net repulsion between pyridine molecules in the

monolayer was characterized by a change in the free energy for monolayer adsorption of only 0.48 kcal/mole. Given the much larger change in adsorption energy of the bilayer, the accumulation of a second layer of polar molecules must play an essential role in stabilizing the charge density of the monolayer.

Quantitation of surface layers. The reproducibility of the sample handling and Raman data acquisition methods can also be exploited to estimate surface concentrations of the pyridine adsorbate. From the linear response region of the 992 cm^{-1} band in Figure 6, the sensitivity of detection can be calibrated against the known solution concentrations. The ratio of the silica surface area to the solution volume within the packed bed is estimated by using the surface area of the silica reported by the manufacturer from standard N_2 BET methods and a chromatographic measurement of the solution volume in a packed column of the same silica gel [4]. The result, 4.1 m^2/l, allows the known solution phase concentration of adsorbate to calibrate the response from molecules on the surface. The calibrated response requires one final correction for changes in the Raman cross section for the totally symmetric ring mode when pyridine is protonated. This correction was determined by comparing the scattering intensity from identical concentrations of pyridine in acidic and basic aqueous solution and by a similar comparison of pyridine and pyridine hydrobromide in chloroform. The Raman scattering cross section of the symmetric ring mode appears to increase slightly, by 11%, upon proton transfer.

With the solution phase pyridine thus acting as an internal standard, the plateau in scattering intensity of the monolayer adsorbate is used to estimate the limiting surface coverage of this species to be $\Gamma = 2.5\ (\pm 0.5)\ \mu moles/m^2$. This result is comparable to the 3.1 $\mu mole/m^2$ surface coverage of the identical silica when reacted with excess trimethylchlorosilane [29], where the yield of

bound silane was determined by carbon analysis. (Note: Both of these surface concentrations are lower bounds [30], since they are reported on the basis of the N_2-BET surface area of the silica). The equivalent surface concentration of adsorbed pyridine relative to this small bound silane infers that pyridine probably does not lie flat on the silica surface. This conclusion is consistent with a Bronsted interaction between the surface and adsorbate, where the lone-pair electrons on the pyridine nitrogen would be oriented toward a surface silanol. The same calibration method was also used to estimate the limiting surface concentration of pyridine in the bilayer to be $\Gamma_b = 0.6\ (\pm 0.1)$ μmoles/m^2. Somewhat surprising is that the limiting number of pyridine molecules in the bilayer is about one fourth that in the monolayer. The actual surface concentration, compared to the monolayer, could be larger if surface area is lost upon adsorption of the monolayer [31]. Even with a fractional loss of surface area, it is interesting that the much smaller number of molecules in a physisorbed bilayer can appear to play a significant role in the energetics of the interface.

Summary. A technique for the acquisition of Raman spectra of molecules adsorbed at the liquid-solid interface has been developed where spectra are collected using low power, red excitation in conjunction with a charge-coupled-device detector. This combination minimizes fluorescence interference from the solid support while providing adequate sensitivity for detecting scattered radiation in the near-infrared region. Samples of porous silica are contained in a flow cell through which solutions are pumped to equilibrate with the silica surface; this approach to sample handling controls the illuminated surface area of the porous silica samples and to minimize background from solution phase species. The resulting control over adsorbate signal leads to

excellent reproducibility, where small deviations from Langmuir behavior can be readily identified, the accumulation of physisorbed bilayers can be detected, and the density of adsorbed molecules on the surface can be determined.

The technique is applied to study the adsorption of pyridine onto silica from carbon tetrachloride solution. Spectroscopic adsorption isotherms are acquired which allow monolayer and bilayer forms of adsorbed pyridine to be distinguished. The monolayer form adsorbs with significant proton transfer from the silica surface, where the degree of proton transfer decreases uniformly with increasing pyridine coverage. The monolayer isotherm data were found to fit a Frumkin model which accounted for the lowering of the free energy of adsorption with increasing surface coverage, in agreement with the observed changes in the degree of proton transfer. The limiting surface density of the monolayer was also determined and found to be consistent with edge-on adsorption of the pyridine ring. The bilayer isotherm exhibited a concentration threshold, which was found to fit a Frumkin-like model where the energy of adsorption increased strongly with increasing monolayer coverage. The accumulation of this second layer of molecules having a higher dielectric constant than the solvent appears play a role in stabilizing the charge density of ion pairs in the monolayer. Studies are underway to compare the adsorption behavior of pyridine to silica under more polar solvent conditions, where a second adsorbate layer would be expected to play a less energetic role in stabilizing the adsorbed monolayer.

ACKNOWLEDGMENT

This work was supported in part by the Office of Naval Research and by Dow Chemical, U.S.A.

REFERENCES

1. Lochmüller, C. H.; Marshall, D. B.; Wilder, D. R. Anal. Chim. Acta, 1981, 130, 31.
2. Lochmüller, C. H.; Marshall, D. B.; Harris, J. M. Anal. Chim. Acta, 1981, 131, 263.
3. Lochmüller, C. H.; Colburn, A. S.; Hunnicutt, M. L.; Harris, J. M. J. Am. Chem. Soc. 1984, 106, 4077.
4. Carr, J. W.; Harris, J. M. Anal. Chem. 1986, 58, 626.
5. Carr, J. W.; Harris, J. M. Anal. Chem. 1987, 59, 2546.
6. Murray, C. A.; Dierker, S. B. J. Opt. Soc. Am. A 1986, 3, 2151.
7. Schlotter, N. E.; Schaertel, S. A.; Kelty, S. P.; Howard, R. Appl. Spectrosc. 1988, 42, 746.
8. Shannon, C.; Campion, A. J. Phys. Chem. 1988, 92, 1385.
9. Campion, A. in "Vibrational Spectroscopy of Molecules on Surfaces"; Yates, J. T., Madey, T. E., Eds.; Plenum Press: New York, 1987; Chapter 8.
10. Witke, K. Appl. Spectrosc. 1982, 36, 471.
11. Sayed, M. B.; Cooney, R. P. J. Colloid Interface Sci. 1983, 96, 381.
12. Strommen, D. P.; Nakamoto, K. "Laboratory Raman Spectroscopy"; Wiley: New York, 1984.
13. Lochmüller, C. H.; Colburn, A. S.; Hunnicutt, M. L.; Harris, J. M. Anal. Chem. 1983, 55, 1344.
14. Bevington, P. R. "Data Reduction and Error Analysis for the Physical Sciences", McGraw-Hill: New York, 1968.
15. Cooney, R. P.; Tam, N. T. Aust. J. Chem. 1976, 29, 507.
16. Hendra, P. J.; Turner, I. D. M.; Loader, E. J.; Stacey, M. J. Phys. Chem. 1974, 78, 300.

17. Schrader, G. L.; Cheng, C. P. J. Phys. Chem. 1983, 87, 3675.

18. Kung, M. C.; Kung, H. H. Catal. Rev. Sci. Eng. 1985, 27, 425.

19. Hendra, P. J.; Horder, J. R.; Loader, E. J. J. Chem. Soc. A, 1971, 1766.

20. Brunauer, S. "The Adsorption of Gases and Vapors", Princeton University: Princeton, NY, 1943.

21. Langmuir, I. J. Am. Chem. Soc. 1918, 40, 1361.

22. Honig, J. M. Ann. New York Acad. Sci. 1954, 58, 741.

23. Frumkin, A. N. Z. Phys. Chem. 1925, 116, 466.

24. Frumkin, A. N.; Damaskin, B. B. in "Modern Aspects of Electrochemistry, No. 3" Bockris, J. O'M.; Conway, B. E., eds. Butterworths: Washington, D.C., 1964.

25. Aveyard, R.; Haydon, D. A. "An Introduction to the Principles of Surface Chemistry", Cambridge: London (1973); Chapter 6.

26. Delahay, P. "Double Layer and Electrode Kinetics", Wiley-Interscience: New York, 1965; Chapter 5.

27. West, R. C., ed. "49th Handbook of Chemistry and Physics", Chemical Rubber Co.: Cleveland, 1968; pp. E-58, E-60.

28. Israelachvili, J. N. "Intermolecular and Surface Forces", Academic Press: New York, 1985; Chapters 3, 4.

29. Hunnicutt, M. L.; Harris, J. M. Anal. Chem. 1986, 54, 748.

30. Farin, D; Avnir, D. in "The Fractal Approach to Heterogeneous Chemistry", Avnir, D., ed., John Wiley: New York, 1989.

31. Unger, K. K. "Porous Silica", Elsevier Scientific: New York, 1979.

FIGURE CAPTIONS

1. Raman spectra of pyridine collected at the carbon tetrachloride/silica gel interface. Bands originating from surface adsorbed pyridine appear initially at 1012 cm^{-1} and 1034 cm^{-1} followed by bands at 992 cm^{-1} and 1030 cm^{-1} which correspond to physisorbed and bulk solution pyridine. Pyridine solution concentrations are from bottom to top: 1.9 mM, 9.6 mM, 19 mM, 96 mM, 0.19 M, 0.96 M, and 1.9 M.

2. Raman spectrum of adsorbed pyridine and corresponding fit to Gaussian band shapes. Solution concentration of pyridine is 96 mM. Peak shape parameters were obtained through minimization of a chi-squared statistic subject to the constraints described in the text.

3. Frequency of totally symmetric ring mode, ν_1, of adsorbed pyridine versus relative surface coverage. The shift in the band from 1012 cm^{-1} to 1008 cm^{-1} indicates a decrease in the charge transfer between the pyridine adsorbate and the silica surface.

4. Spectroscopic isotherm of pyridine adsorbed at the carbon tetrachloride-silica interface. The scattering intensity of the totally symmetric ring mode, ν_1, of adsorbed pyridine (points) is scaled and plotted versus the solution concentration of pyridine. A best fit to a Langmuir isotherm over the range of 0.96 mM - 0.57 M is plotted (solid line). (a) Linear concentration scale over a limited range of 0 - 0.96 M; (b) logarithmic concentration scale to illustrate the quality fit over the entire range, 0.96 mM - 0.57 M.

5. Spectroscopic isotherm for pyridine adsorbed to silica, fit to Frumkin model (Equation 3). (a) Linear concentration scale over a limited range; (b) logarithmic concentration scale over the entire fitted range.

6. Plot of 992 cm^{-1} Raman band intensity versus pyridine concentration. In the linear region of the curve at high pyridine concentrations, the signal is dominated by Raman scatter from pyridine in bulk solution. The non-linear region includes signal originating from a bilayer of adsorbed pyridine, the intensity of which is the difference between the points and the extrapolated line.

7. Bilayer isotherm for pyridine on silica. Points are derived from the results in Figure 6 (see text). Solid line is the best fit to the bilayer model of Equation 4.

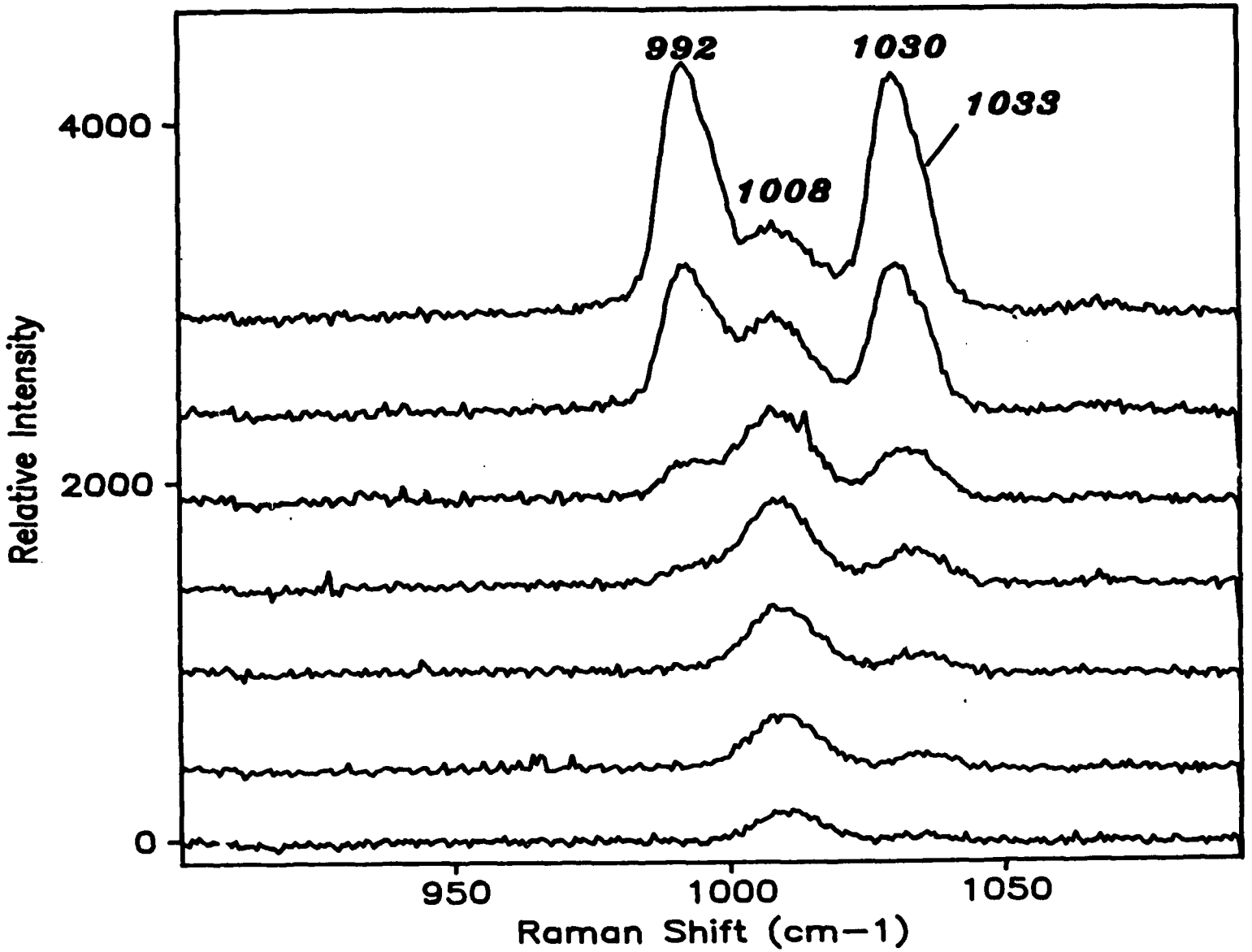
992
1030
1033
1008
4000
2000
0
Relative Intensity
950
1000
1050
Raman Shift (cm−1)

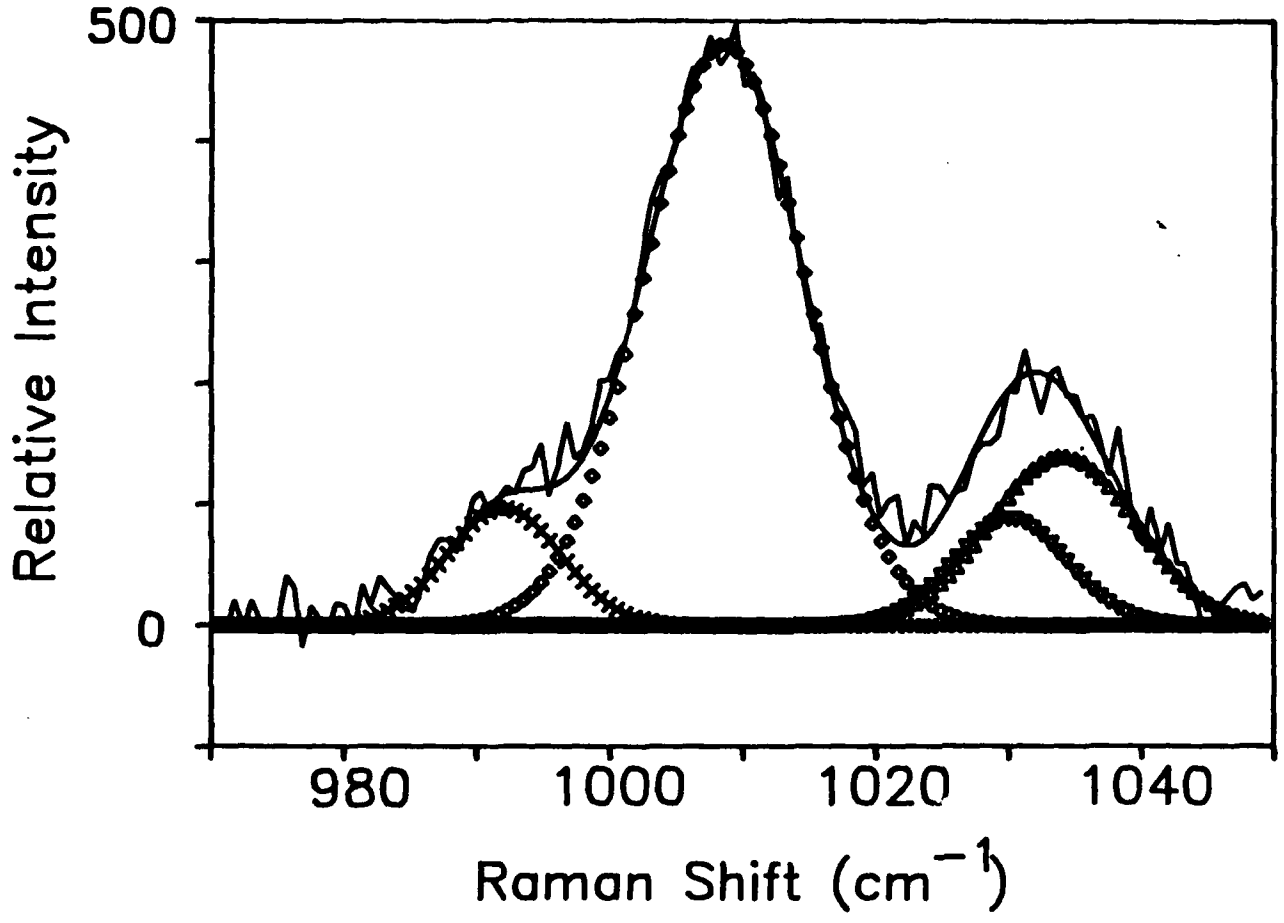

Figure 2

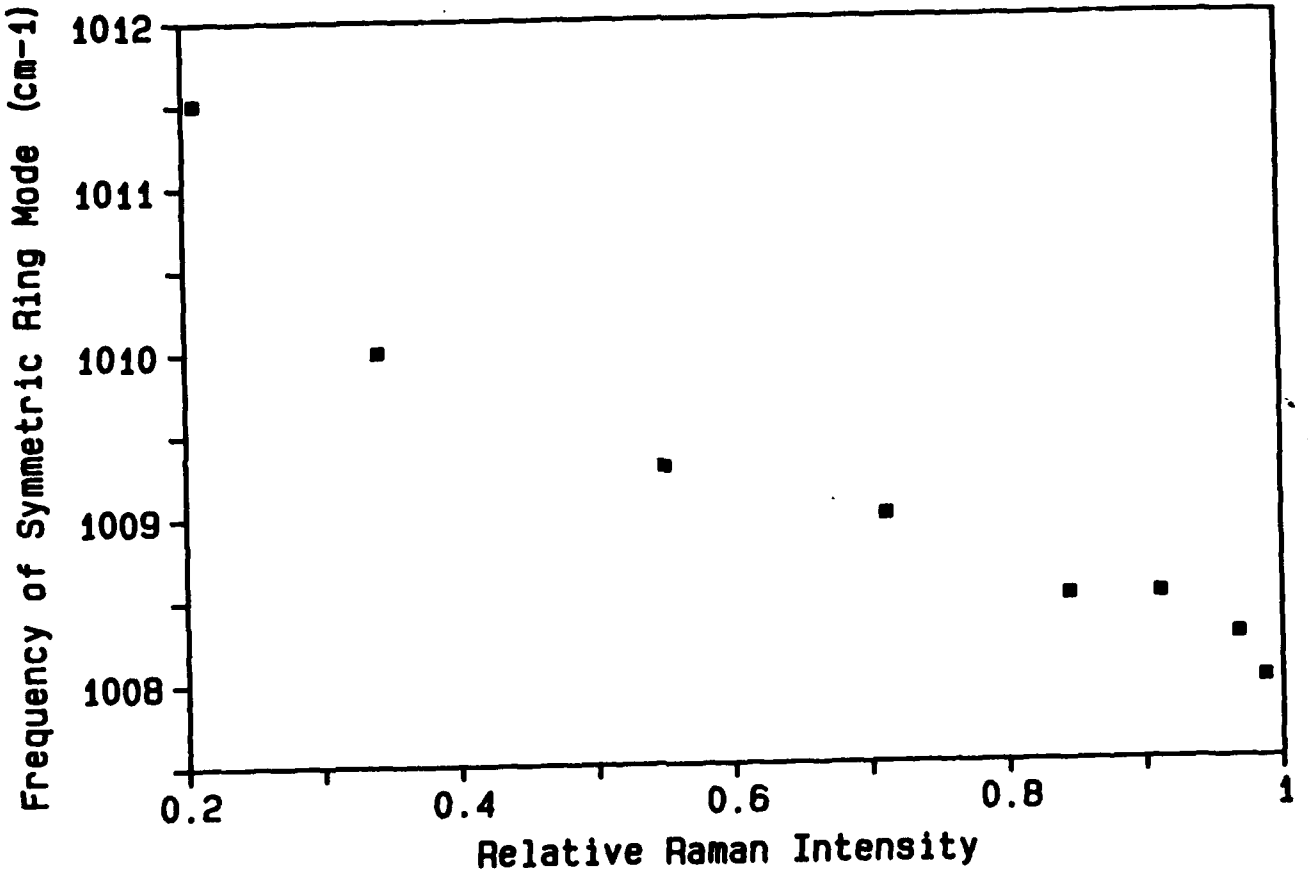
Frequency of Symmetric Ring Mode (cm-1)
1012
1011
1010
1009
1008
0.2
0.4
0.6
0.8
1
Relative Raman Intensity

Figure 3

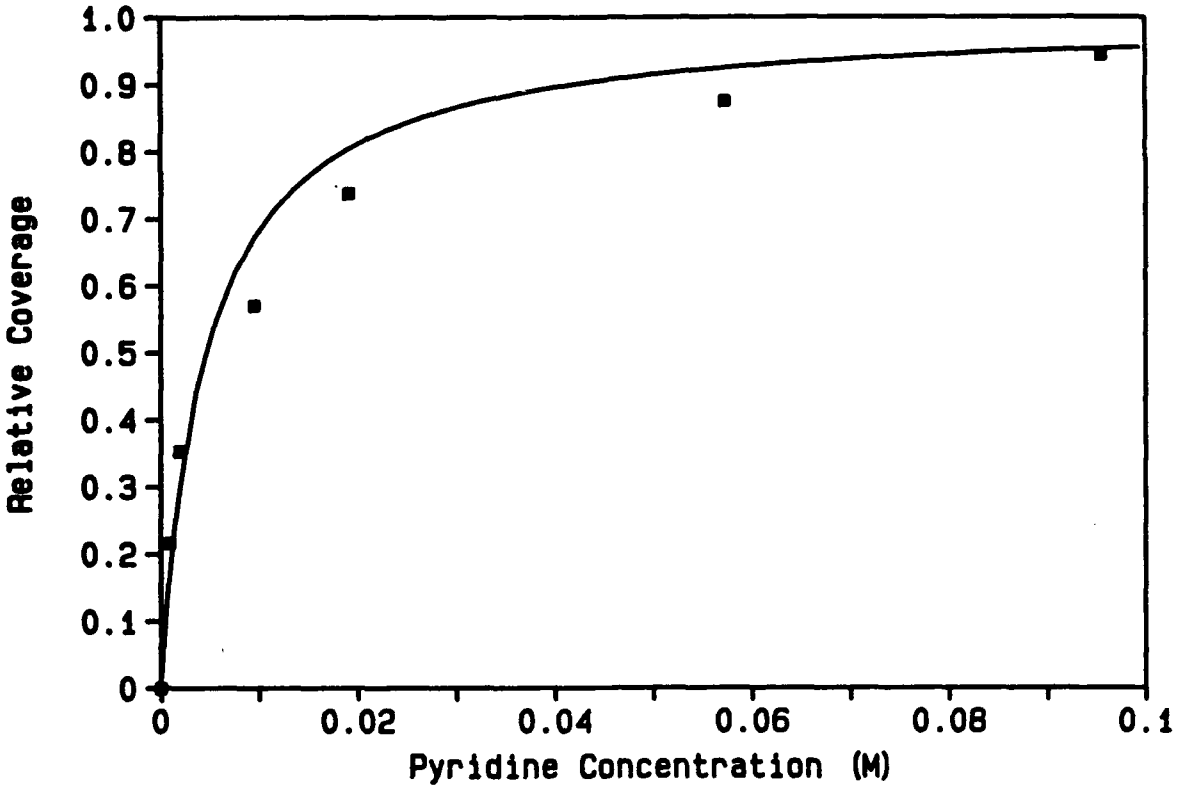
1.0
0.9
0.8
0.7
0.6
0.5
0.4
0.3
0.2
0.1
0
Relative Coverage
0
0.02
0.04
0.06
0.08
0.1
Pyridine Concentration (M)

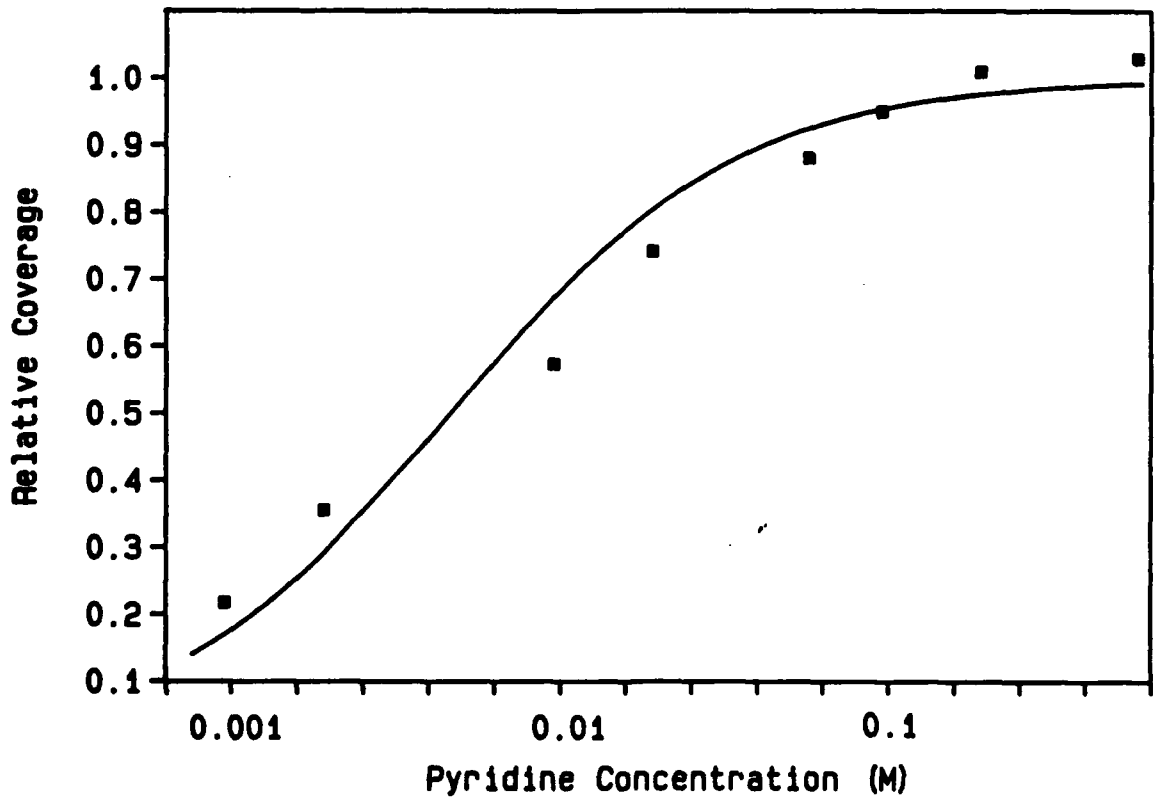
1.0
0.9
0.8
0.7
0.6
0.5
0.4
0.3
0.2
0.1
Relative Coverage
0.001
0.01
0.1
Pyridine Concentration (M)

Figure 4

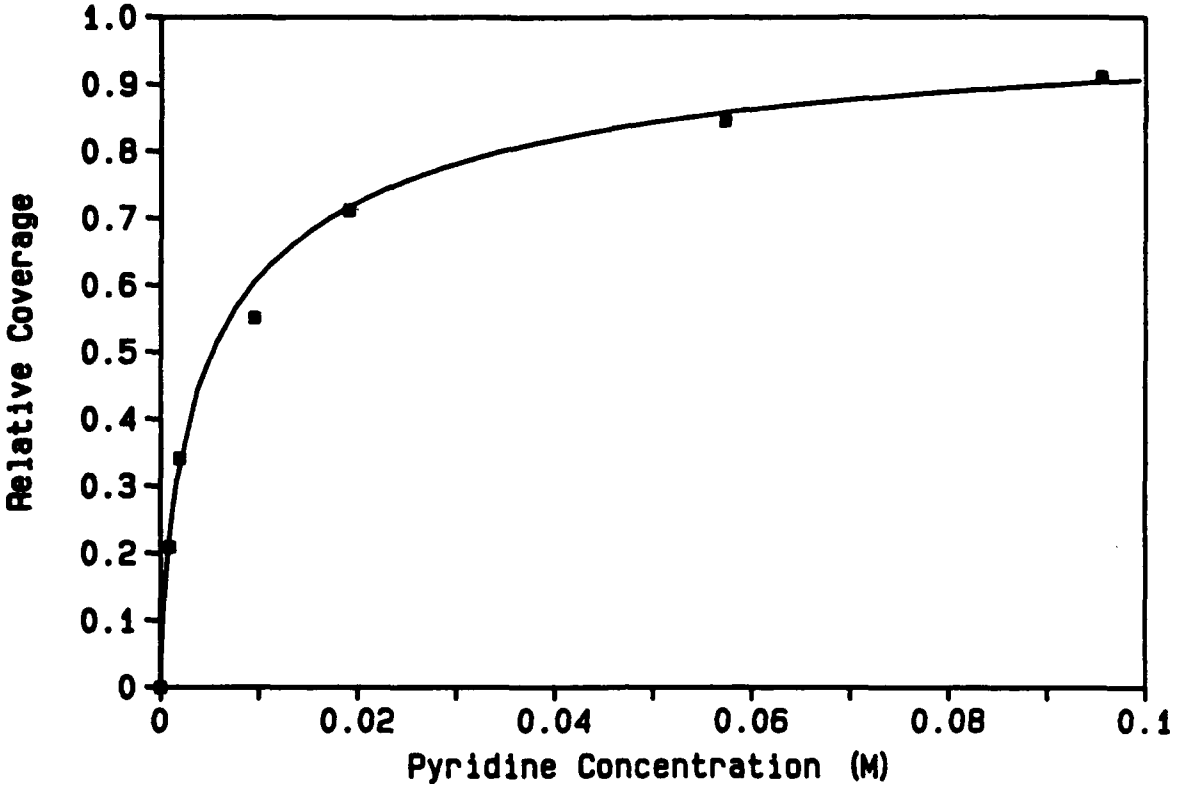
1.0
0.9
0.8
0.7
0.6
0.5
0.4
0.3
0.2
0.1
0
Relative Coverage
0
0.02
0.04
0.06
0.08
0.1
Pyridine Concentration (M)

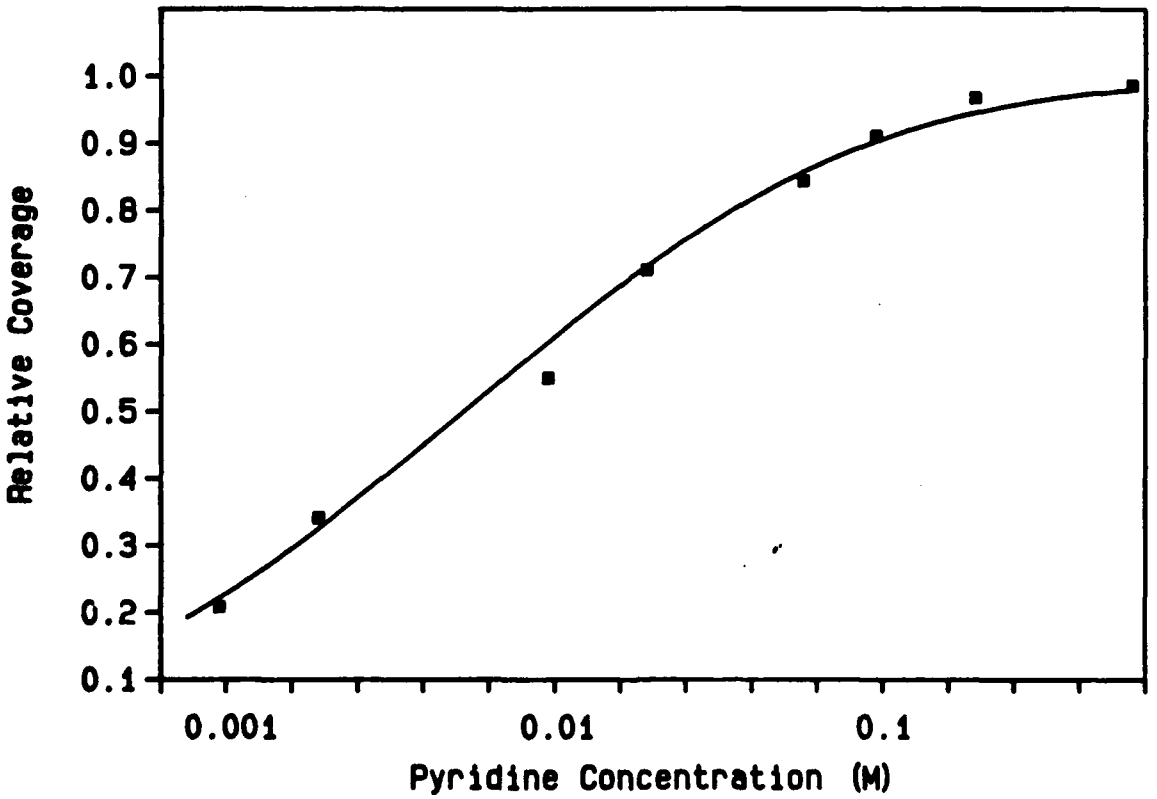
1.0
0.9
0.8
0.7
0.6
0.5
0.4
0.3
0.2
0.1
Relative Coverage
0.001
0.01
0.1
Pyridine Concentration (M)

Figure 5

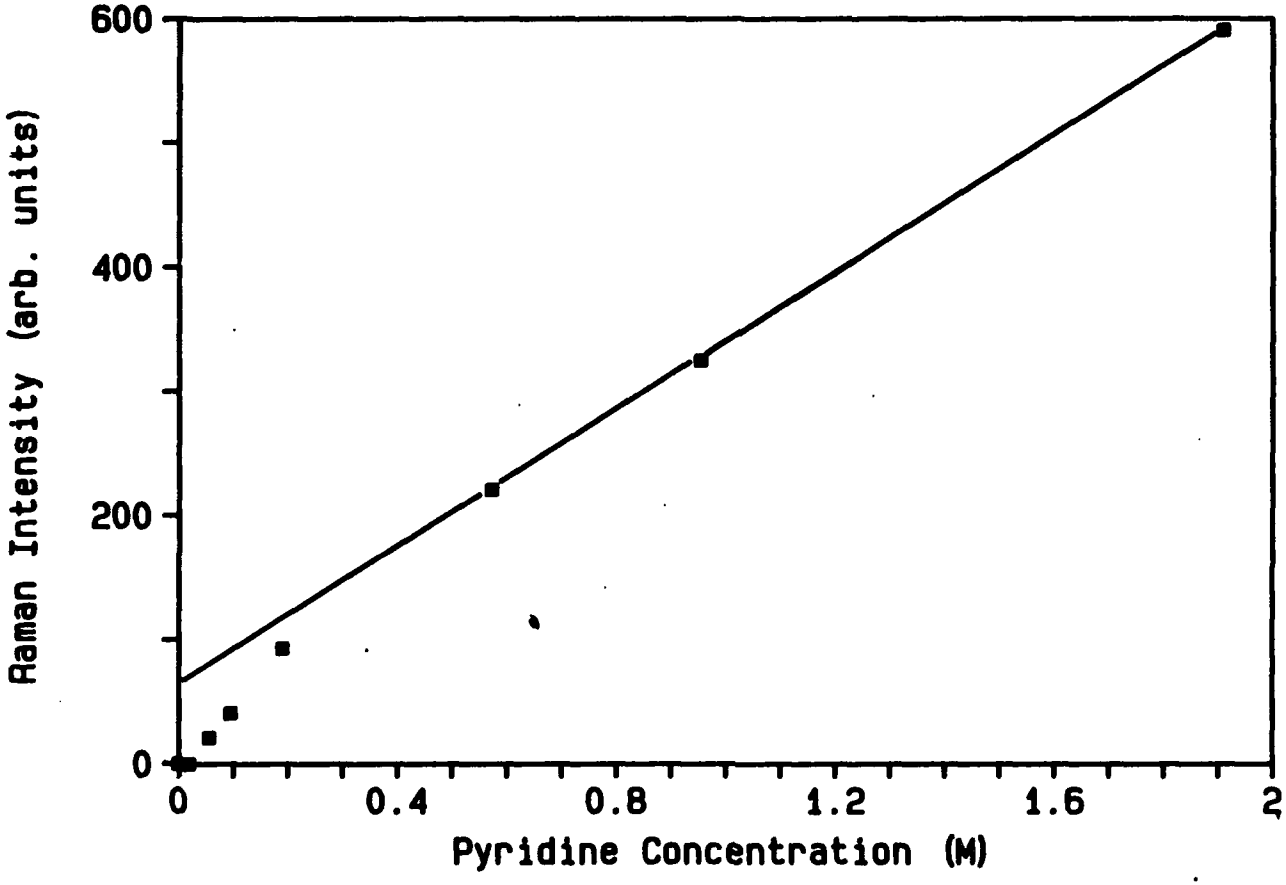
600
400
200
0
Raman Intensity (arb. units)
0
0.4
0.8
1.2
1.6
2
Pyridine Concentration (M)

Figure 6

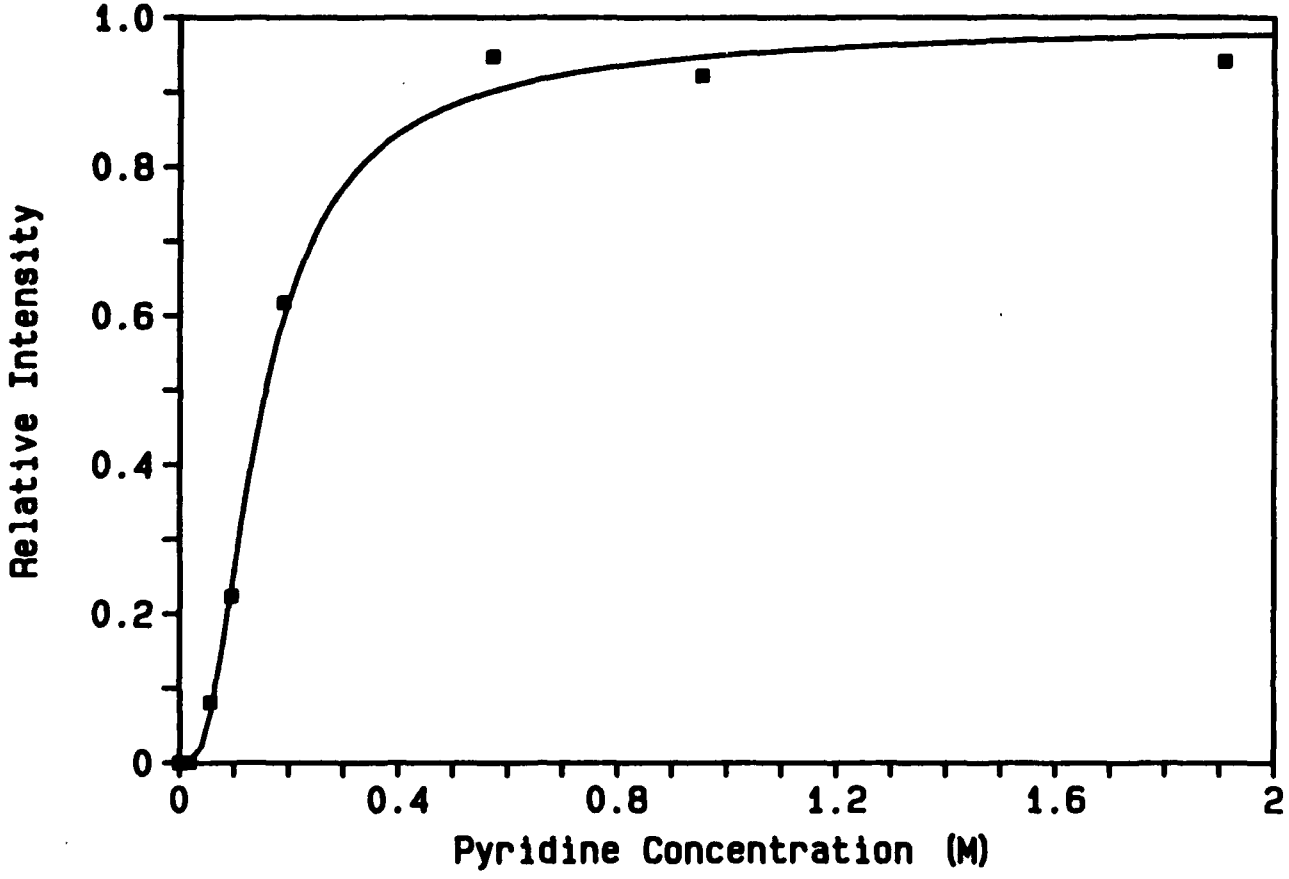
Relative Intensity
1.0
0.8
0.6
0.4
0.2
0
0
0.4
0.8
1.2
1.6
2
Pyridine Concentration (M)

Figure 7